AIAA 82-4143

Laser-Induced Fluorescence Visualization on Supersonic Mixing Nozzles That Employ Gas-Trips

August A. Cenkner Jr.* and Richard J. Driscoll†
Bell Aerospace Textron, Buffalo, N. Y.

A laser-induced iodine fluorescence visualization technique has been refined and used extensively to study supersonic cold-flow mixing. In particular, visualization studies were performed in the mixing region between supersonic slit nozzles that employed gas trips for enhanced mixing. The nozzles were operated with room-temperature helium under simulated chemical laser flow conditions. The primary objective was to develop insight into the trip-enhanced mixing phenomenon. Three-dimensional information was therefore acquired on the size, shape, location, structure, and interaction of the primary, secondary, and trip jets under both trip-on and trip-off operation. This has led to postulations on the existence of three trip-induced convective mechanisms that appear to contribute to enhanced mixing. The active mechanisms, as well as the dominant mechanism, appear to depend upon: the type of trip configuration used, the nozzle width, and the flowfield location since one mechanism appears to dominate in the primary nozzles and another in the secondary nozzles.

Introduction

A CHALLENGING engineering problem of current concern is that of reactant injection/mixing in continuous flow combustion devices, such as: chemical rocket and jet engines, furnaces, and chemical lasers. In these devices, unmixed reactants are continuously fed independently through different nozzles into a chamber where reactant mixing and combustion occurs. Subsequent to the extraction of power, the combustion products are continuously exhausted. It has been found that the mixing process has a major impact on the performance of the device. For this reason, a considerable amount of time has been spent on improving the mixing process; see for example Refs. 1 and 2.

A relatively new approach for enhancing reactant mixing, and hence improving device efficiency, is the use of gas-trips in the mixing nozzles. This technique entails the injection of nonreacting gas through small orifices that are installed in the side walls of the mixing nozzles near the exit plane. The idea, as one theory goes, is to trip prematurely the transition from laminar flow. In the area of high-energy chemical lasers, the use of gas-trips in supersonic slit nozzles has resulted in more than a doubling of the laser power. Infrared radiometer scans of the mixing cavity confirmed that the trips had caused the combustion to occur at a faster rate.[3] Unfortunately, optimization of the gas-trip approach was inhibited by a lack of a clear understanding of how the gas trips interact with the reactant flow to produce the increased performance.

This experiment was undertaken to acquire basic information on trip nozzles, using simulated laser flow, to help develop an understanding of the trip-enhanced mixing phenomenon. Toward this objective, a considerable amount of information was acquired on the mixing region characteristics of four different trip nozzle arrays, for both trip-off and trip-on operation. This included automated pitot probe scans, laser Doppler velocimeter measurements,[4] and flow visualization using laser-induced fluorescence of a selectively seeded iodine vapor. Due to space limitations, only representative data will be presented for the BCL-18 nozzle.

Received May 18, 1981; revision received Nov. 2, 1981.

*Scientist, High Energy Laser Technology. Member AIAA.
†Group Leader, Laser Fluid Mechanics. Member AIAA.

At present no basic gasdynamic literature is available on mixing nozzles that utilize gas trips, hence it is of interest to consider an area that has some bearing on the problem: gas jet injection from a circular hole (or pipe) into a crossflow.[5-11] While these works were primarily directed toward problems associated with atmospheric phenomena, fuel injection into combustors, attitude control rockets, thrust vector control, etc., they also provide some insight into the anticipated behavior of isolated trip jets.

References 5-7 address subsonic transverse injection of a single (initially) circular jet into a uniform lower velocity subsonic stream. The main features of interest here include flow behavior that in many ways resembles that of flow across a solid cylinder. These features include: the crossflow is decelerated as it approaches the upstream jet boundary and it is deflected upward and sideward around the jet; high- and low-pressure regions are respectively established upstream and downstream of the jet; and, in general, vortices are periodically shed into the wake region. In contrast to flow about a solid body though, the flow exhibits distinctive behavior including: the nonuniform peripheral pressure distribution results in a change in the original circular cross-sectional shape of the jet; the jet is deflected downsteam; and a mixing region is formed in the boundary of the jet. Also, for a given crossflow momentum, the centerline of the jet (i.e., the maximum velocity locus) expands further into the flow as the jet momentum is increased. Flow behavior is more complex when the secondary wall jet is injected into a supersonic cross stream.[8-11] Flow obstruction by the jet now results in the formation of a shock wave. Interaction between this shock and the wall boundary layer results, in general, in a separation of the boundary layer, which further alters the jet boundary pressure distribution.

Experimental Arrangement

A small stainless steel slit nozzle array was fabricated for this activity. The array (designated BCL-18) is shown in Fig. 1, while details of the nozzle design are presented in Fig. 2. With three contoured secondary nozzles and two contoured primary nozzles, the array is 1.778 cm wide and 1.270 cm long. Three small tubes are used to side feed the secondary distribution tubes from a common cylindrical reservoir that is located on the right side of the nozzle block. Through 10 staggered rearward facing orifices, each distribution tube in turn feeds a secondary plenum chamber. The six gas-trip manifolds are side fed, through six small tubes, from a

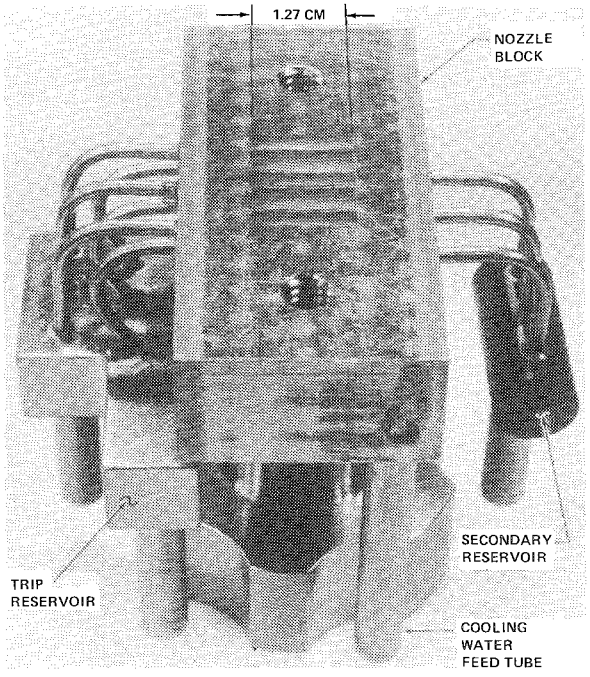

Fig. 1 BCL-18 laboratory nozzle array.

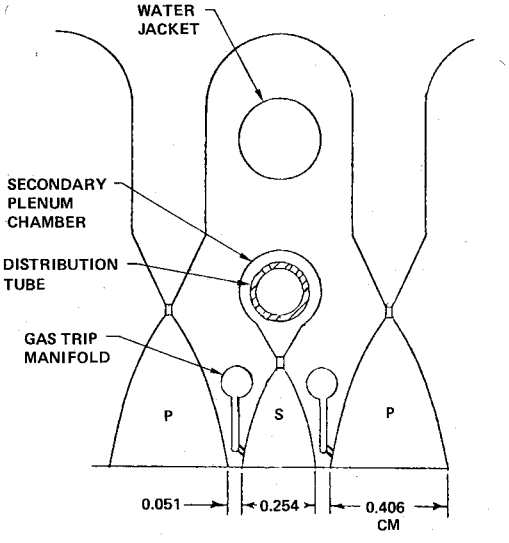

Fig. 2 BCL-18 nozzle design.

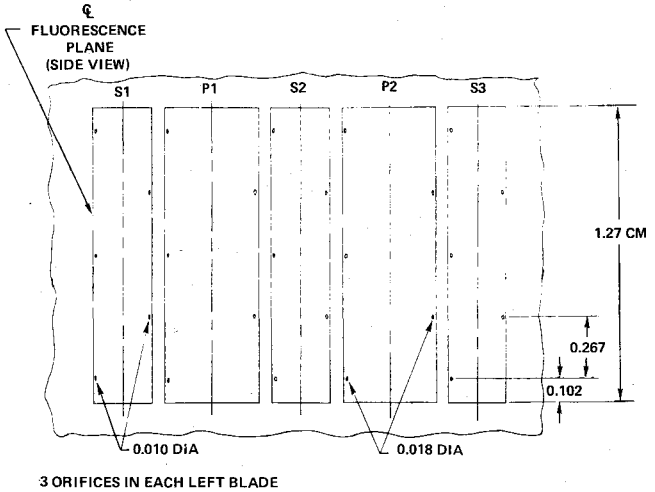

Fig. 3 Nozzle trip pattern 2.

Table 1 BCL-18 test conditions

Primary nozzle	
Plenum pressure	873 kPa
Plenum temperature	293 K
Flow rate	3.46 g/s
Gas	Helium
Secondary nozzle	
Supply pressure[a]	1296 kPa
Supply temperature	293 K
Flow rate	2.03 g/s
Gas	Helium
Gas trips	
Supply pressure[a]	704 kPa
Supply temperature	293 K
Total flow rate	0.18 g/s
	0.10 g/s
Gas	Helium
Cavity	
Pressure	2.67 kPa

[a] Upstream of distribution orifice in nozzle.

common reservoir located to the left of the nozzle block. In contrast, the primaries are back fed in common by a 1.905 cm (i.d.) tube. Water jackets in the nozzle block, for nozzle cooling during hot firings, are fed through the small tube at the front corner of the nozzle block. For discussion purposes, the secondary and primary nozzles are respectively numbered from top to bottom as S1, P1, S2, P2, and S3.

Supply pressures and temperatures for the secondaries and the trips are monitored at the inlet to their respective reservoirs. These supply pressures do not correspond to the plenum pressures because of a substantial pressure drop across the choked orifices located inside the nozzle block. Primary plenum pressure and temperature are measured at the inlet to the 1.905 cm feed tube. Calibrated sonic orifice flow meters were used for all flow rate measurements. Gas temperatures were determined from direct-reading thermocouples that were protruding into the flow.

Gas-trip orifice sizes and spacings of the reported pattern are given in Fig. 3 for both the primary and secondary nozzles. All of the orifices were inclined at 45 deg relative to the nozzle axes.

The nozzle array was centered in an 8.89 cm i.d. test section during all testing. This was to insure free-jet operation of the jet array. Room-temperature helium was used throughout as the test gas; operating conditions are given in Table 1.

Fluorescence Visualization

A laser-induced iodine fluorescence visualization technique was recently demonstrated on an HF chemical laser.[12] This technique was refined herein and used extensively during supersonic cold-flow mixing studies.

In this technique, the fluid stream of interest is seeded with molecular iodine vapor. The flowfield is then locally illuminated by a green (514.5 nm) argon ion laser beam to pump the I_2 to an excited electronic energy level. When the excited iodine spontaneously decays to an intermediate energy level, yellow fluorescence is emitted. When it then decays to an even lower level, red fluorescence appears. If a narrow-band optical filter is used to block the green pumping beam, a planar cross section of the fluorescing stream can be observed or recorded using standard electro-optical or photographic techniques.

This technique is attractive for a number of reasons, including the fact that it is relatively easy and inexpensive to implement. By controlling the size of the pumping beam, high- or low-spatial resolution can be selected as required. Mutual interaction between gas streams can be studied through consecutive independent seeding of each stream. Also, for exploring complex three-dimensional flows, planar cross-sectional slices can be taken at any desired location or orientation. Combined, these capabilities allow for acquiring

an extensive amount of three-dimensional information on the size, shape, location, structure, interaction, and intermixing of gas streams.

With respect to the control of spatial resolution, a number of different schemes can be used. One approach uses a beam expander to enlarge the pumping beam. A sheet of light is then formed by inserting a slit into the beam path. With an alternate method, a focusing lens is used to reduce the beam diameter. The fluorescing plane is then recorded as the beam is translated across the field of view. If a shorter field of view is required, the beam can, of course, be held stationary. Generation of a sheet of light by a cylindrical lens would also be appropriate.[13] The selected approach depends upon a number of considerations: physical constraints imposed by test section designs, accessibility, availability of components, etc.

It is worth commenting on a number of potential problem areas that should be taken into account before adopting this fluorescence visualization technique. For instance, background window fluorescence, where the laser beam penetrates the test section windows, and high-intensity fluorescence reflections can become a nuisance but are easily overcome with judicious design and masking when recognized (not always easy to detect when recording with black-and-white film). Natural fluorescence of the optical filter or other optical components, on the other hand, has not proved to be a problem. The incompatibility of iodine with many materials, along with its tendency to freeze-out in flow passages (and eventually plug small orifices), are probably the most constraining considerations. Although the passages are easily cleaned with acetone or alcohol, the cleaning has to be fairly frequent. Heating of the flow passages or superheating of the iodine vapor does help reduce the freeze-out problem. Not to be overlooked is the effect of iodine on any mechanical equipment. Some small standard valves, for example, eventually freeze shut. Over an extended period, iodine adversely affected the vacuum pump performance by coating the internal surfaces and contaminating pump oil; however, cleaning and oil changing did appear to restore the pump. In some applications, it may be desirable to remove the iodine gas from the flow before it enters any mechanical devices. This could be accomplished through the use of screens, gauze, or cold traps.

Test Procedure

Two configurations were used, during this sequence of tests, for recording the fluorescence. In the first, as illustrated in Fig. 4, the flow was observed from the side of the nozzle. The nozzle blades were oriented with 1.27 cm length horizontal so that an extended length of the mixing zone could be studied. Three front surface mirrors were used to steer the laser beam to a vertical orientation. The beam was then allowed to diffusely scatter from the blackened upper surface of the test section. Mirror M1, being about 3.810 cm long, was mounted directly to the bottom of the nozzle block. Mirrors M2 and M3 were both mounted to a common axial translation stage. By using a stepper motor to move this mounting stage, it was possible to automatically translate the vertical laser beam over the entire mirror length. This effectively rendered visible a planar slice through the flowfield that had a width equal to the beam diameter. When gross spreading characteristics were of interest, the beam was left at its normal 0.164 cm diam. If it was desired to look at more localized phenomena, a lens was inserted and the beam diameter was reduced to about 0.025 cm. Inasmuch as the nozzle array length is 1.270 cm, the gross spreading perspective afforded by the larger beam is integrated over about 12% of the flow, while probing by the smaller beam would be restricted to about 2% of the flow.

A question naturally arises about the stability of the flow structure while the flow was being scanned by the laser beam. To the eye, the primary and secondary streams, as well as the trip jets, all appear to be steady.

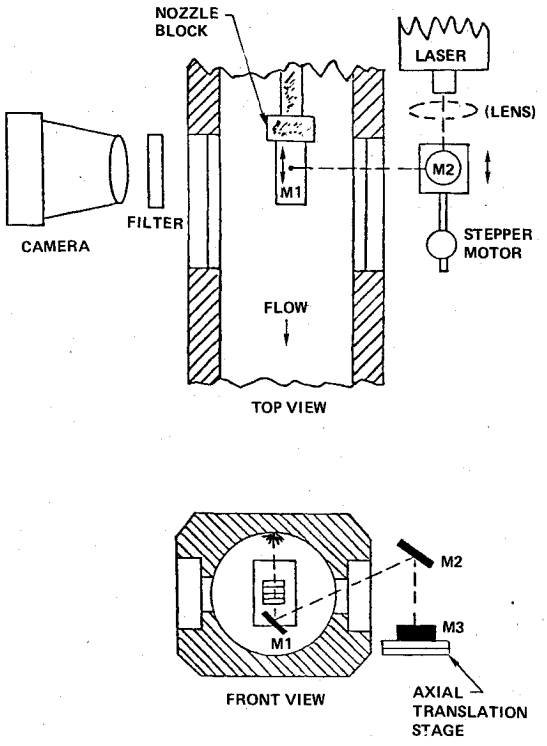

Fig. 4 Fluorescence photography test setup, side view.

A major concern was the protection of the silvered front surface of the M1 beam steering mirror, which is located inside the test section, since it was exposed directly to the iodine gas. A helium gas curtain effectively protected the mirror; however, such an approach could not be used since it adversely affected the flow from the nozzle. When cleaned every hour or so, the mirror survived without the gas curtains; however, the iodine destroyed the silvered surface during more extended testing.

In this first configuration, the fluorescing plane was recorded on color film (Kodacolor 400) by a 35 mm camera that was positioned on the side of the nozzle. The shutter was held open while the beam was repeatedly translated back and forth for several minutes, thereby forming an image of a planar slice of the flow. A narrow bandpass optical filter (centered at 575 nm) was required for filtering the green pumping beam. To eliminate background illumination by stray light, all work was performed in a darkened laboratory. For initial focusing of the camera, a small probe was temporarily installed in the test section at the beam position.

In the second configuration (Fig. 5), the flow was observed from a downstream vantage point that was 45 deg off the nozzle axis. This required a reconfiguration of the optical system. Mirrors M2 and M3 were oriented so that the laser beam now passed horizontally across and parallel to the nozzle face. With the stepper motor now driving a transverse translation stage, the horizontal beam was translated vertically. This in effect cut a cross-sectional slice through the flow at a given axial location. By translating the test section in the upstream direction, it was possible to slice the flow at any desired axial location while maintaining each slice at the camera focal point. All of the photographs that were taken with this 45 deg view employed the 0.025 cm diam beam. However, the visible-plane width is larger than this if the fluorescence relaxation times are longer than the local characteristic supersonic flow times.

A Spectra-Physics Model 165 argon ion laser, operating with 0.2 W output power, served as the illumination source. An etalon was installed in the laser so that the laser could be tuned for maximum fluorescence at the test section operating pressure. Etalon tuning is critical since the iodine will not fluoresce if the etalon is improperly tuned.

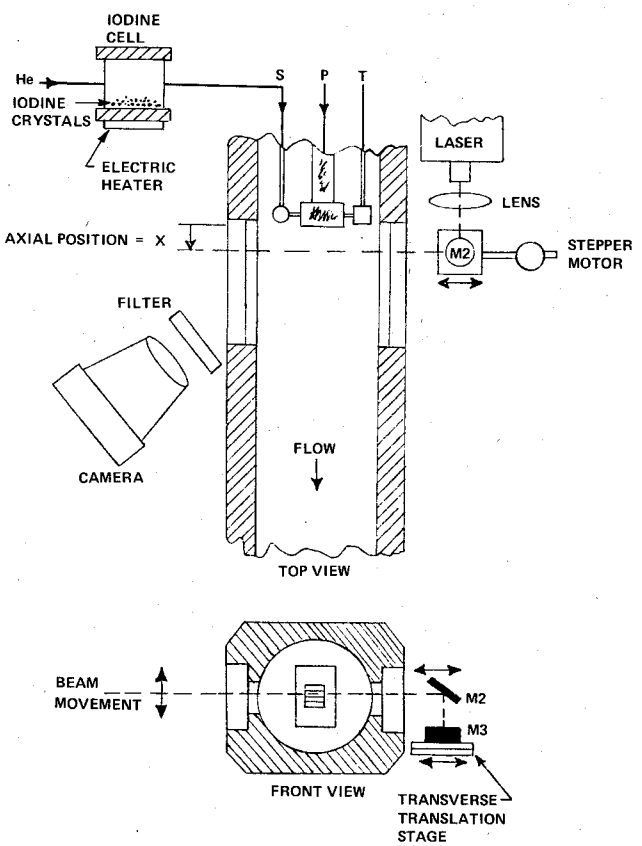

Fig. 5 Fluorescence photography test setup, 45 deg view.

A small cell that served as the iodine vapor source was installed as shown in Fig. 5. The cell was comprised of an 8.89 cm diam plexiglas cylinder, 6.350 cm long, with metallic end plates. For protection from the iodine, these plates were coated with Teflon since the uncoated aluminum plates became severely pitted. A thin-foil electrical heater was bonded to the outside surface of the lower plate so that the iodine concentration could be increased by increasing the plate temperature. A thin layer of subliming crystals was uniformly spread on top of the lower plate. The test gas for a given circuit was diverted through the cell in order to entrain the iodine vapor. The cell was switched between flow circuits as required. When the cell was removed from one circuit, it was necessary to bleed gas through the lines to remove residual iodine from that circuit. The 0.64 cm diam feed line between the cell and the nozzle block was a flexible stainless steel tube with a Teflon liner. Unlined stainless steel tubing showed pitting after use. Initially, a small hand valve was installed between the iodine cell and the nozzle. After this valve froze shut, isolation of the cell was achieved by removing the feed line and capping off the cell. At flow rates higher than those reported herein, the helium carrier gas was observed to swirl in the plexiglas iodine cell, thereby entraining some of the iodine crystals. During some tests a metal screen filter was, therefore, installed between the cell and the nozzle. The plexiglas housing of the iodine cell discolored during use but was not attacked.

As would be expected, a thin iodine film eventually built up on the test section windows. But, it was found that this film did not etch the quartz windows. Film formation was precluded by using gas curtains in front of the windows; heating of the windows would also have been effective. Excessive use of gas curtains for providing protection from iodine had one major drawback. It increased the gas load to the vacuum system, thereby increasing the vacuum pressure, in some cases to an unacceptable level.

Both stainless steel and aluminum nozzles were successfully used for test periods of several hours without any obvious surface degradation. The stainless steel nozzle did begin pitting during more extended testing.

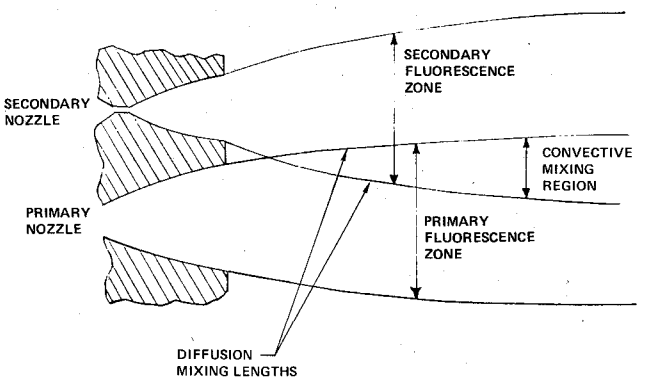

Fig. 6 Comparison between fluorescence zones, convective mixing region, and mixing lengths.

Results and Discussions

In order to study the interaction between the primary, secondary, and trip streams, the same region of the flow was probed by the laser while the iodine seeding was switched from stream to stream. As illustrated in Fig. 6, the overlapping region established by the primary and secondary fluorescence zones then defines the convective mixing region—the region where the primary and secondary gases would be convectively intermixed. It should be pointed out that this overlapping may not in general identify the full extent of the mixing region. If the dominant mixing mechanism is convective in nature, then it is reasonable to expect that the common fluorescence region is the same as the test gas mixing region. But, if molecular diffusion contributes significantly to the mixing process, then the test gas mixing region will be underestimated. This is because of the dependency of the molecular diffusion coefficient on collision cross sections and on the molecular weights of the mixing gases. For this study, since He molecules are so much lighter and smaller than I_2 molecules, the molecular diffusion contribution to mixing would be understated. However, the length of the boundaries of the convective mixing region give a direct indication of the extent of additional mixing by molecular diffusion. In this study, the ability to isolate convective mixing from diffusion mixing has been a definite advantage.

Side view photographs of the untripped secondary jets, obtained with the 0.152 cm wide laser beam positioned as indicated in Fig. 3, are presented in Fig. 7a. Corresponding tripped behavior is given in Figs. 7b and 7c. A 0.025 cm diam beam was used in acquiring the 45 deg views of Figs. 8 and 9. In some cases, fine flow features are more evident in the original color negatives than in the black-and-white reproductions introduced herein.

Since the intent of this study is to use a small nozzle array (1.27×1.778 cm) to study the interaction between a typical primary/secondary nozzle pair in a much larger array, attention should be mainly focused on the middle of the secondary jet S2 and the two adjacent primary jets (P1 and P2). These jets are shielded on the side from boundary effects by S1 and S3 and are, therefore, more representative of typical jets in a large nozzle array. The vertical dark streaks that appear in the downstream region of Fig. 7 are the result of iodine attacking the M1 beam steering mirror.

This side view of the trip-off secondary jets in Fig. 7a exhibits a number of interesting features:

1) One of the most striking features is the flow direction change in the width of the secondary jets. This is due to oblique (or curved) shock waves being reflected from the jet boundary. To verify this conclusion, pitot probe scans were

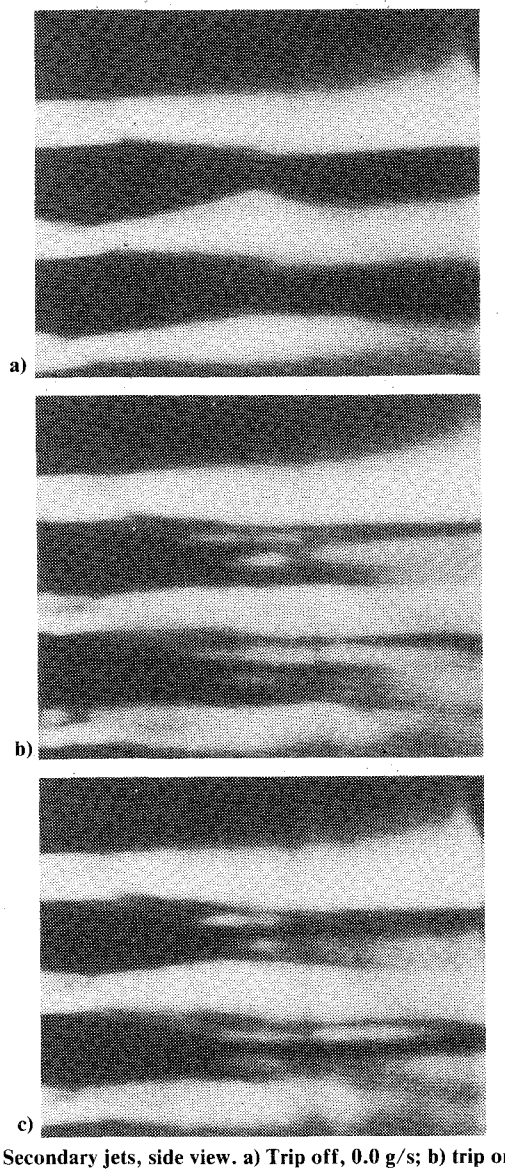

Fig. 7 Secondary jets, side view. a) Trip off, 0.0 g/s; b) trip on, 0.18 g/s; c) trip on, 0.10 g/s.

made at numerous axial locations. Large pressure spikes, characteristic of oblique shocks, were detected in both the primary and secondary streams at locations as close as 0.76 mm to the nozzle face. Similar spikes were reported in Ref. 3. The BCL-18 shock waves are no doubt the result of off-design operation of these contoured nozzles. This is indicated by the closeness of the shocks to the nozzle face and by the fact that the shocks in the primary streams persisted when the secondary streams were turned off and the secondary shocks persisted when the primary streams were turned off, i.e., they are not primary/secondary interaction shocks.

2) In the observed field of view, the fluorescence zones never penetrate to the centerline of the adjacent primary stream.

3) Near the nozzle face, the free (outer) and confined (inner) jet boundaries are rather distinct, thereby indicating an abrupt change in iodine concentration. Further downstream the confined boundaries retain this appearance but the free boundaries become more nebulous, an indication of a more significant transverse dispersion of the seeded iodine. This suggests a difference in spreading intensity or different spreading mechanisms that may be related to a higher shear region along the free boundary that leads to transition from laminar flow. Further support for this contention is the fact that when the primary and secondary jets were independently operated as free jets this longitudinal change in iodine dispersion was detected along all of the free boundaries.

4) Relatively well-defined dark streak patterns have been detected in much of the primary and secondary jet photography. For example, in the untripped secondary jets of Fig. 7a left and right running streaks, that may be associated with the oblique shocks, are visible near the nozzle face. These dark streak patterns may be indicative of: variations in integrated intensities due to variations in iodine concentration, pressure, and/or velocity; pressure/temperature dependency of the absorption coefficient; and/or refraction effects due to changes in the index of refraction.

When the gas trips are turned on (see Figs. 7b and 7c), there is very little enhanced spreading of the secondaries near the nozzles. Downstream there is significant enhancement, with the secondary streams eventually spreading to the centerline of the primary streams. A jet core, that resembles the original trip-off jet, is now separated from a boundary region by dark horizontal streaks. These boundary regions are actually the local "protrusions" that were detected in the 45 deg views, which will be discussed shortly. When the gas trip flow rate is reduced from 0.18 to 0.10 g/s, there is a corresponding reduction in the downsteam depth of penetration of the secondary streams into the primary streams.

Cross-sectional slices were taken of the flow at three different axial locations (0.0, 0.76, and 1.52 cm from the nozzle face), while the flow was observed from a 45 deg downstream vantage point (see Figs. 8 and 9). The dark horizontal streaks that appear in many of the 45 deg photographs are due to irregular movement of the laser beam. The normally used stepper motor had malfunctioned so the laser beam was translated manually. It should be recalled, if attempting to make exact measurements from these 45 deg photographs, several things result in one-dimensional distortions: the 0.025 cm width of the laser beam, and the elongation of the fluorescing plane when the characteristic supersonic flow time is shorter than the fluorescence relaxation time.

At 0.0 cm, in Figs. 8a and 8b, the left and right sides of the trip-off primary and secondary jets are concave due to overexpanded operation. That is, these boundaries are being compressed by a cavity pressure that is higher than the jet exit pressure. The other jet boundaries are not distorted because of transverse momentum associated with the nozzle divergence. A narrow structured boundary region is evident around the periphery of an apparently unstructured core in both the primary and secondary jets (0.0 and 0.76 cm). This apparently unstructured core could possibly be related to the film being overexposed to the point that core structure is obscured. Numerous small fingerlike projections develop on the facing (constrained) boundaries of the primaries and the secondaries at 0.76 cm. The (free) side boundaries of all jets, as well as the (free) side boundaries of the S1 and S3 jets, do not exhibit the fingerlike projections. At 1.52 cm the primary jets appear to have developed a core structure.

Consider now the same region of the flow when the trips are turned on. From Fig. 8c, near the nozzle face, the trip jets behave like solid deformable bodies. They are solid in the sense that they retain their identities as discrete entities and they are deformable in the sense that their size and shape are dependent upon operating conditions. In general, the cross sections of the secondary trip jets are crescent shaped in appearance while the irregular primaries sometimes resemble the letters U or H, presumably because of a nonuniform pressure distribution. Moving downstream to 0.76 cm, the secondary trip jets begin breaking up and eventually spread to the extent that they no longer can be identified. In contrast, the primary trip jets retain their identity, grow in size, and develop an internal structure at 0.76 cm. At the 1.52 cm station, boundary effects produce breakup of the outer primary trip jets while the three inner P1 and P2 jets retain their identity. It does appear, however, that the middle P1 and P2 trip jets have been compressed at this station. Notice that

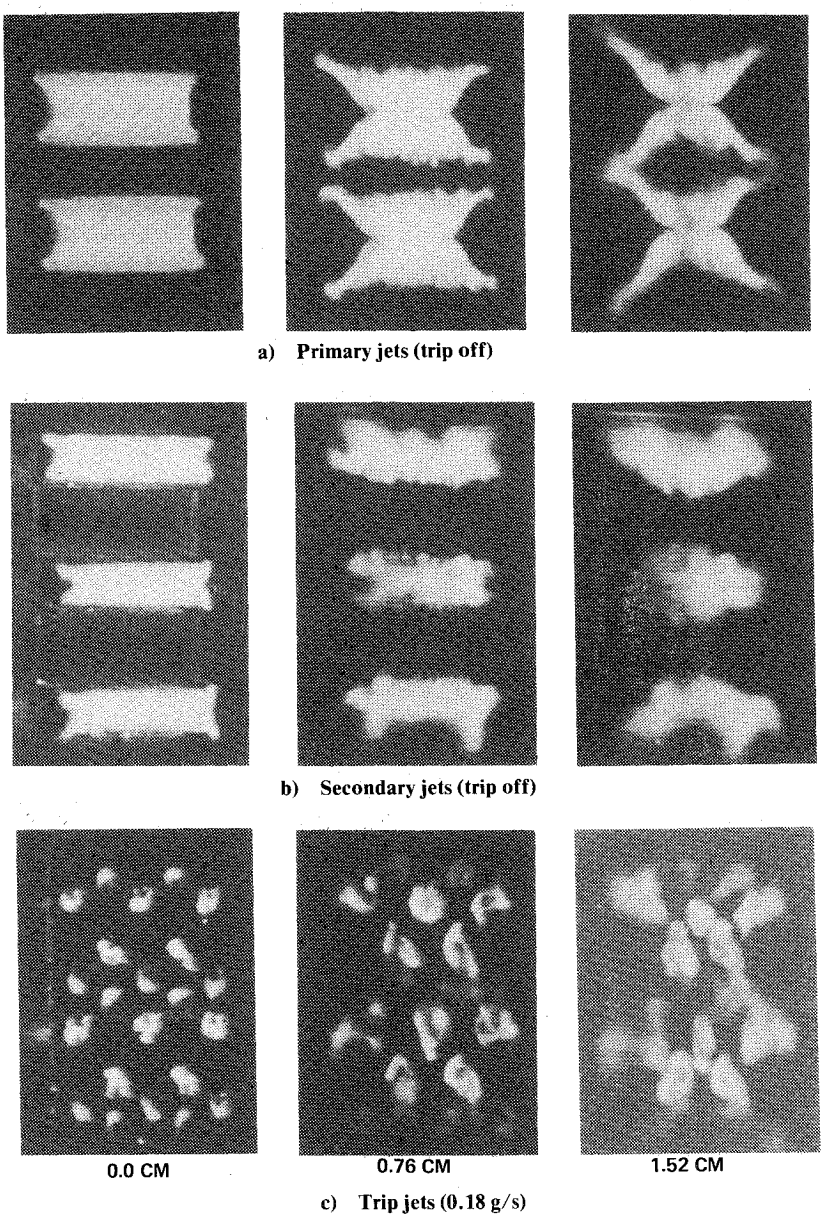

Fig. 8 Fluorescence zones, 45 deg view.

the complete breakup of typical primary and secondary trip jets, i.e., jets that are shielded from edge effects, occurs at different axial locations. This distinctive behavior suggests that the differences in primary and secondary nozzle widths (0.406 vs 0.254 cm) and/or the differences in trip orifice sizes (0.018 vs 0.010 cm) leads to premature breakup of the secondary trip jets, possibly because of an interaction between adjacent jets.

Both the trip-on primary and secondary streams, at the 0.0 cm station in Figs. 9a and 9b, show black voids embedded in the jets. With the exception of the S1 nozzle, there are three of these voids near the top boundaries and two near the bottom. Comparison with the nozzle trip orifice pattern of Fig. 3 and the corresponding fluorescing trip jets of Fig. 8c reveals that these voids are the (cores of the) unseeded trip jets; the trips have displaced regions of the main streams. Primary and secondary boundary undulations between these voids are due to the expansion of the unseeded trip jets from the adjacent nozzle. Notice the apparent structure in the high-shear region between the primary stream and the black voids of the trip jets. By comparing the sizes of the black void regions and the corresponding fluorescing trip jets, it can be seen that there is a trip-gas/main-flow mixing region in the boundary of the trip jet, in addition to an unmixed trip core. At 0.0 cm, there is very little difference in the widths of the trip-on and trip-off primary and secondary jets. This shows that the nozzle flow was not separated from the nozzle walls by the trip jets.

The 0.76 cm primary and secondary cross sections give the first real clues, so far, to the identity of the trip-induced mechanisms that cause enhanced spreading/mixing of these jets. By comparing these views with the corresponding trip-off cross sections of Fig. 8, it is obvious that both the trip-on primary and secondary jets have spread by a greater amount. It is also obvious that their spreading behavior is different. The secondary streams have very localized spreading, via relatively large distinct fingerlike protrusions that extend far into the primary streams. In contrast, the primary streams spread more uniformly along the length of the nozzle. It will be recalled that the convective mixing region is identified by the overlapping of these primary and secondary fluorescence zones.

When the gas trip flow rate is reduced from 0.18 to 0.10 g/s, the sizes of the near nozzle trip jets are reduced but their shapes appear to remain unchanged; compare Figs. 8c and 9c at 0.0 cm. From Figs. 9b and 9d at 0.76 and 1.52 cm, it can be seen that the localized protrusions of the secondary streams also decrease in both size and penetration depth.

Based partially on the findings of the literature search presented in the Introduction, the following interpretation evolves. Consider first the localized protrusions of the trip-on

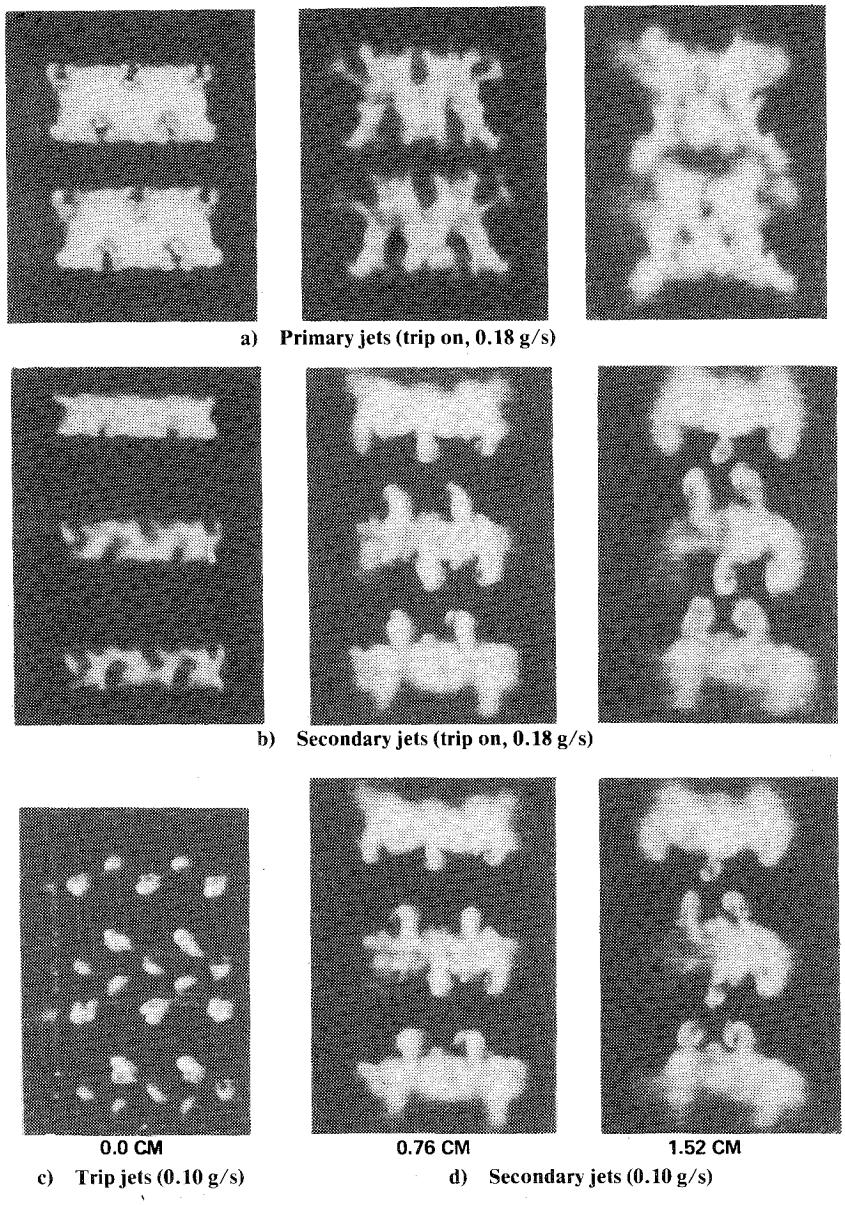

Fig. 9 Fluorescence zones, 45 deg view.

secondary streams into the primary streams. These protrusions could be related to the solid-body-like behavior of the primary trip jets near the nozzle face. Basically, the solid-body-like obstruction of the primary streams by the trip jets in the primary nozzles creates a low-pressure region on the downstream side of the trip jets. This low-pressure wake draws flow from the adjacent secondary stream into the primary stream, with the possible assistance of local higher pressure regions in the secondary streams that are produced by the secondary trip jets. Vortices and/or turbulence in the high-shear region between the trip and the primary stream could then spread the drawn secondary flow around the trip jets. Let us now attempt to make a qualitative correlation between this postulation and some of the experimental results. From Figs. 8c, 9b, and 9d at the 0.76 and 1.52 cm stations, the secondary protrusions correspond to the locations of the primary trip jets. At the 0.76 cm station some of the protrusions have a small knob near the apex. At the 1.52 cm station this knob seems to have expanded so that it now completely encircles a black void (trip jet core). Based on these photographs, there appears to be qualitative agreement between the proposed interpretation and the data acquired with this trip pattern. As a point of interest, consider the localized protrusions that extend from the lower (free) boundary of the bottom S3 jet at 0.76 cm in Figs. 9b and 9d under trip-on conditions. This, at face value, appears to contradict the proposed theory since there are no trip jets to "draw out" this gas. The apparent discrepancy can be resolved by considering the corresponding trip-off axial position in Fig. 8b. The protrusions exist even under trip-off operation, so, they are a manifestation of the natural expansion of the jet array and are not related to the trip jets.

The more uniform spreading of the primaries, as compared to the secondaries, could be accounted for in a number of different ways. The breakup of the secondary trip jets could introduce enough of a disturbance into the secondaries so that they "nibble away" at the primary streams. Or, the spreading could be related to primary stream pressure response to the solid-body behavior of the trip jets. To see how this would occur, recall that it was shown earlier that the trip jets displace regions of the main flow. Because of this displacement, as well as because of the close proximity of the jets, local regions of the main flow are compressed. If the trips create localized high-pressure regions in the primaries, this could cause the primaries to expand laterally into the adjacent secondaries. Secondary trip jet breakup may then assist spreading. To test this main stream high-pressure buildup hypothesis, gas trips were installed only in the secondary nozzles. Fluorescence visualization and pitot probe scans showed that the secondary jets expanded both lengthwise and transversely into the primary streams. This behavior tends to support the pressure buildup hypothesis. It also demonstrated that, at least with

that particular trip configuration, the secondary main stream was not being "drawn out" by the primary trip jets because there were no primary trip jets.

One final observation: consider the trip-off and trip-on primary jet cross section at 0.76 and 1.52 cm. In particular, compare the concave side boundaries and the length of the primary jets at the middle of the nozzles. Notice that when the trips are turned on the jets expand and the boundaries become less concave. This indicates that there is a trip-induced pressure buildup in the primary streams that prevents these streams from being compressed as much as they are when the trips are off. The secondary streams appear to behave in a similar manner but the effect does not appear to be as pronounced.

It is of interest to compare these results with the laser Doppler velocimeter (LDV) measurements that were reported in Ref. 4, even though the measurements were made on a different nozzle. It was found that the trip-off wake turbulent intensity (rms/mean velocity) never exceeded 10% for measurements that were made out to a distance of 2.29 cm from the nozzle face. When the trips were turned on, the maximum turbulent intensity did not increase. Rather, the (low-level) turbulence in the wake of the base region was spread into the core of the nozzles. This appears to be consistent with the visualization results that show that the secondary streams (and turbulence) are being locally drawn into the primary streams by the primary trip jets.

In the LDV study, it was also found that there was a local increase in the rate at which particles cross the LDV measurement volume, when the gas trips were turned on. This could be explained by an increase in the particle concentration as the flowfield pressure increased. The mean velocity did not increase so velocity changes were ruled out as a cause.

Conclusions

Basic information was acquired on the gas-trip-enhanced mixing of supersonic slit nozzles. Three convective mechanisms have subsequently been proposed as contributing to enhanced mixing of adjacent gas streams: 1) the low-pressure wake of the "solid body" trip jets "draws" gas from the adjacent secondary flow; 2) a high-pressure region is established in the nozzle main flow, by the trip jets in the same nozzle, which "pushes" this main flow into the adjacent stream; and 3) trip-jet breakup which may trigger a nibbling/spreading effect on the adjacent main flow or which may work in conjunction with the second mechanism. Which mechanisms are active, as well as which mechanisms dominate, appears to depend upon: the type of trip configuration used, position in the flowfield, and nozzle size.

Flow behavior associated with the injection of gas-jet arrays, from opposing sides of a small nozzle into a supersonic stream, have been found to differ in a number of ways from that associated with injection of an isolated jet. The pressure in the main stream increases when the jets displace significant regions of the main flow, which can lead to a lateral expansion of the main flow. Interaction between the injected jets probably results in a premature breakup of these jets. In addition, the size, shape, and position of individual jets in the array are probably altered somewhat from those of the isolated injected jet.

This work has demonstrated the usefulness of employing fluorescence visualization in mixing studies. The next step in the development of this diagnostic method should be the utilization of a computerized electro-optical system for data acquisition so that more quantitative information can be obtained. This would allow for an accurate measurement of the extent of the convective mixing region and the diffusional mixing length (Fig. 6), as well as sizes and locations of the jets.

Acknowledgments

The authors would like to express their appreciation to G. W. Tregay for numerous discussions on chemical lasers, for suggestions that were related to the cold flow testing, and for reviewing the original manuscript. This work was supported under Air Force Weapons Laboratory Contract F29601-77-C-0007 and under corporate IR&D programs.

References

[1] Kennedy, L. A. (ed.), *Progress in Astronautics and Aeronautics: Turbulent Combustion,* Vol. 58, AIAA, New York, 1978.

[2] Summerfield, M. (ed.), *Progress in Astronautics and Aeronautics: Injection and Mixing in Turbulent Flow,* Vol. 68, AIAA, New York, 1980.

[3] Gross, R. W. F. and Bott, J. F., "The Flowfield in a Mixing-Laser Cavity," *Handbook of Chemical Lasers,* John Wiley and Sons, New York, 1976, pp. 301, 338-341.

[4] Cenkner, A. A. Jr., "Laser Doppler Velocimeter Measurements on Supersonic Mixing Nozzles that Employ Gas-Trips," *AIAA Journal,* Vol. 20, March 1982, pp. 383-389.

[5] Pantankar, S. V., Basu, D. K., and Alpay, S. A., "Prediction of the Three-Dimensional Velocity Field of a Deflected Turbulent Jet," *Journal of Fluids Engineering,* Dec. 1977, pp. 758-762.

[6] Kamotani, Y. and Greber, I., "Experiments on a Turbulent Jet in a Cross Flow," *AIAA Journal,* Vol. 10, Nov. 1972, pp. 1425-1429.

[7] Moussa, Z. M., Trischka, J. W., and Eskinazi, S., "The Near-Field in the Mixing of a Round Jet with a Cross-Stream," *Journal of Fluid Mechanics,* Vol. 80, Pt. I, June 1977, pp. 49-80.

[8] Schetz, J. A., Hawkins, P. F., and Lehman, H., "Structure of Highly Underexpanded Transverse Jets in a Supersonic Stream," *AIAA Journal,* Vol. 5, May 1967, pp. 882-884.

[9] Schetz, J. A. and Billig, F. S., "Penetration of Gaseous Jets Injected into a Supersonic Stream," *Journal of Spacecraft and Rockets,* Vol. 3, Nov. 1966, pp. 1658-1665.

[10] Zukoski, E. E. and Spaid, F. W., "Secondary Injection of Gases into a Supersonic Flow," *AIAA Journal,* Vol. 2, Oct. 1964, pp. 1689-1696.

[11] McClinton, C. R., "The Effect of Injection Angle on the Interaction Between Sonic Secondary Jets and a Supersonic Free Stream," NASA TN D-6669, Feb. 1972.

[12] Rapagnani, N. L. and Davis, S. L., "Laser Induced I_2 Fluorescence Measurements in a Chemical Laser Flowfield," *AIAA Journal,* Vol. 17, Dec. 1979, pp. 1402-1404.

[13] Merzkirch, W., *Flow Visualization,* Academic Press, New York, 1974, p. 35.